CMS TN/95-131
September 1995

Study of the T0 Cathode Strip Chamber Prototype at FNAL

N. Bondar*, D. Eartly, G. Mitselmakher, O. Kiselev*, O. Prokofiev*
Fermi National Accelerator Laboratory, Batavia, IL 60510, USA

A. Korytov
Massachusetts Institute of Technology, Cambridge, MA 02139, USA

S. Durkin, J. Hoftiezer, M. Johnson, P. Lennous, T. Y. Ling, C. Rush
Ohio State University, Columbus, OH 43210, USA

A. Bujak, L. Gutay, D. Human**, R. Lee**
Purdue University, West Lafayette, IN 47907, USA

R. Bernhard**
Valparaiso University, Valparaiso, IN 46863, USA

Abstract

A two-layer Cathode Strip Chamber prototype for the CMS Endcap Muon System has been constructed and tested at FNAL. The results of chamber characteristic measurements with cosmic rays are presented in this paper.

* Visitor from St. Petersburg Nuclear Physics Institute, Russia
** Summer student at FNAL

1 Introduction

The cathode strip chamber (CSC) will be used in the CMS Muon Endcap detector to provide high precision coordinate measurements and bunch crossing identification. The Endcap detector will consist of a system of more than 600 six-layer trapezoidal CSCs. The largest chambers will have a maximum strip length of 3.2 m and a maximum wire length of 1.3 m. As a part of the Endcap Muon R&D program, we have built a small CSC prototype (T0) of 1.5 m (wire direction) x 0.6 m (strip direction) dimensions to evaluate specific aspects the CSC design and to investigate the chamber performance.

2 Chamber Construction

The two-layer T0 CSC prototype (Fig. 1) was constructed from flat aluminum honeycomb panels sandwiched between two skins of copper-clad FR-4 with printed circuit boards. One anode wire plane was placed on each side of the middle panel. The top plane had 30 μm diameter wires (LUMA), the bottom plane had 50 μm diameter wires (SYLVANIA). Two different wire diameters were used to compare chamber characteristics. The anode wires were ganged together in groups of twenty with ten groups per plane. The spacing between the wires was 2.54 mm. Guard strips were placed on the edges of the anode planes. To prevent electrostatic wire instability due to the length of the wires (1.3 m), we installed a FR-4 support bar running across the middle of the anode plane. Cathode strips were machined on the face of one the 3.2 mm thick FR-4 board. The strips were 12.1 mm wide and the spacing between strips was 0.6 mm. This was done for the 30 μm plane only. The other 50 μm plane was constructed without cathode strips to test the new strip technology and its effect on chamber performance. The cathode-cathode gap was 9.52 mm.

3 Experimental Set-up

Fig. 2 shows the experimental set-up used for testing the CSC with cosmic rays. The 20 cm block of iron served to reject soft muons. The signals from the three scintillators were put into coincidence and served as the trigger for measurements. The coincidence count rate of cosmic rays was about 0.8 muons / sec at an angle range of about $\pm 10^{\circ}$.

A schematic view of the electronic set-up is shown in Fig. 3. A 4-channel amplifier/shaper with a fast discriminator [1] was connected to the anode wires. The shaper had a peak time of about 30 nsec. The nominal gain of the anode channels was 3 mV/fC. The amplifier had two different types of discriminators: a zero-crossing and a leading-edge. The two types of discriminators were tested to determine which would be better for timing measurements. The threshold level of the leading-edge discriminator was set to 30 mV. An analog output from the amplifier was used for amplitude measurements and a digital ECL pair timing pulse output was used for timing measurements. The cathode strip read-out electronics consisted of a 16-channel gasplex amplifier/shaper [2] and CAMAC gasplex/ADC controller [1]. The sample and hold time on the gasplex board was set about 400 nsec in order to assure maximum linearity. The ADC had 10 bits with a full scale of 1 V, which corresponds to a charge of 200 fC. Nominal gain of the system was 5 mV/fC, or 0.2 fC/count.

Using this set-up, timing and amplitude measurements were performed for a wide range of voltages. Data was taken for each experimental point for 30-60 minutes. For all testing, we used a gas mixture of 50% CO_2 + 30% Ar + 20% CF_4.

4 Measurements and Results

The CSC was tested from 3.6 kV to 4.3 kV for the 30 μm wire plane and from 4.6 kV and 5.2 kV for the 50 μm wire plane. Fig. 4 shows typical timing and amplitude spectrums of the anode signals from the CSC.

The dependence of anode amplitude on high voltage was measured and the results are shown in Fig. 5. It can be seen that the two planes have equal gas gain when the voltages are 0.8 kV apart. The scale was calibrated to absolute units of charge by taking into account that only about 25% of the total charge on the anode wire is collected by the fast amplifier with the 30 nsec peaking time.

Gas gain uniformity was measured (Fig. 6) to check gap variations in the chamber. The four separate positions of the scintillator counter and the 10 groups of wires creates a grid of 4 x 10 points of measurements with an area of 5 cm x 30 cm per point. These points were plotted in a histogram to estimate gas gain distributions. We found that the gas gain values are contained within ± 30% which corresponds to ± 0.4 mm in full gap variation.

Cross talk between the anode channels was measured. We chose events which occupy only one ADC channel and compared the amplitude from this channel with the

amplitude of neighboring channels (one on the left and one on the right). The ratio spectrum of these events is shown in Fig. 7. As we see from this picture, the level of cross-talk is approximately 3.5%.

We measured the single layer efficiency of the CSCs for both planes and the results are shown in Fig. 8. The efficiency plateau for the 30-μm plane reaches nearly 100% between 3.9 kV and 4.3 kV, and the plateau for the 50-μm plane is between 4.7 kV and 5.2 kV. At these voltage ranges, the peak posistion of the anode amplitude spectrum varied from 0.3 pC to 1.5 pC.

The time characteristics of the CSC for both the zero-crossing and leading-edge discriminators were studied. Fig. 9 shows the dependence of peak position and time resolution, in terms of RMS, on high voltage. We observed that the time resolution for both types of discriminators was nearly equal to 7 nsec at the end of the voltage range. For the zero-crossing discriminator, the peak position and the RMS did not change with voltage. However, for the leading-edge discriminator, a range of 40 nsec was observed in the peak position and the RMS ranged from 7 nsec to 13 nsec as the voltage was varied.

The beam-crossing interval at LHC will be approximately 25 nsec. Fig. 10 shows the efficiency for one CSC plane in a 20 nsec time window. This data was obtained from the time histograms where we defined the number of events in a 20 nsec window and compared this value to the total number of entries. It was found that the chamber was approximately 80% efficient over the entire range in high voltage for the zero-crossing discriminator. The leading-edge discriminator, on the other hand, varied in efficiency from 50% to 85% depending on the voltage.

The induced charge distribution on the cathode strips was monitored from the gasplex controller directly on a digital oscilloscope. For each event (triggered from the scintillator counters) we measured the maximum amplitude from the strips. This was done for 100 events for each voltage, from 3.5 kV to 4.3 kV, for the 30-μm plane. The distributions of the maximum amplitudes for various voltages are shown in Fig. 11. From this data, we estimated the efficiency of the cathode strip read-out by comparing the number of non-overflow events to the total number of events for each voltage. The results are shown in Fig. 12. As we can see from this graph the efficiency is around 98%, below 3.8 kV, but then decreases. For example, if one uses an operation point of 3.9 kV, where charge distribution from the cathode strips is optimum for the dynamic range of the gasplex amplifier, the efficiency drops almost 15%. On the other hand, the anode plateau efficiency, which is also plotted on this figure, begins at 3.9 kV. From this graph it follows that the combined voltage operation range for both anode and cathode electronics is about 100 V. To extend the operational range we must decrease the

threshold of the anode amplifier, (which may be difficult due to the electronic noise from the chamber), or to increase the dynamic range of the gasplex/amplifier controller.

4 Conclusion

The T0 CSC prototype has been constructed and tested. A new technological process involving the machining of cathode strips was used. There were no problems observed in chamber operation with the machined cathode strips.

The time characteristics of the CSCs were investigated for both zero-crossing and leading edge discriminators. Single layer time parameters were better and more stable for zero-crossing discriminator.

We found that the combined operation range for both the anode and the cathode readout electronics is relatively small and further investigations are needed to define optimal sensitivity and dynamic range of the anode and cathode electronics.

5 Acknowledgments

We would like to thank the following people for their input and assistance:
P. Deering, K. Gray, A. Gordeev, K. Kephart, J. Korienek, N. Michael, S. Pordes.
We are also grateful to all the members of the Endcap Muon group for their numerous discussions and suggestions.

References

1. Ohio State University Electronics group.
2. J. C. Santiard et al., CERN-ECP/94-17, CERN preprint, 1994.

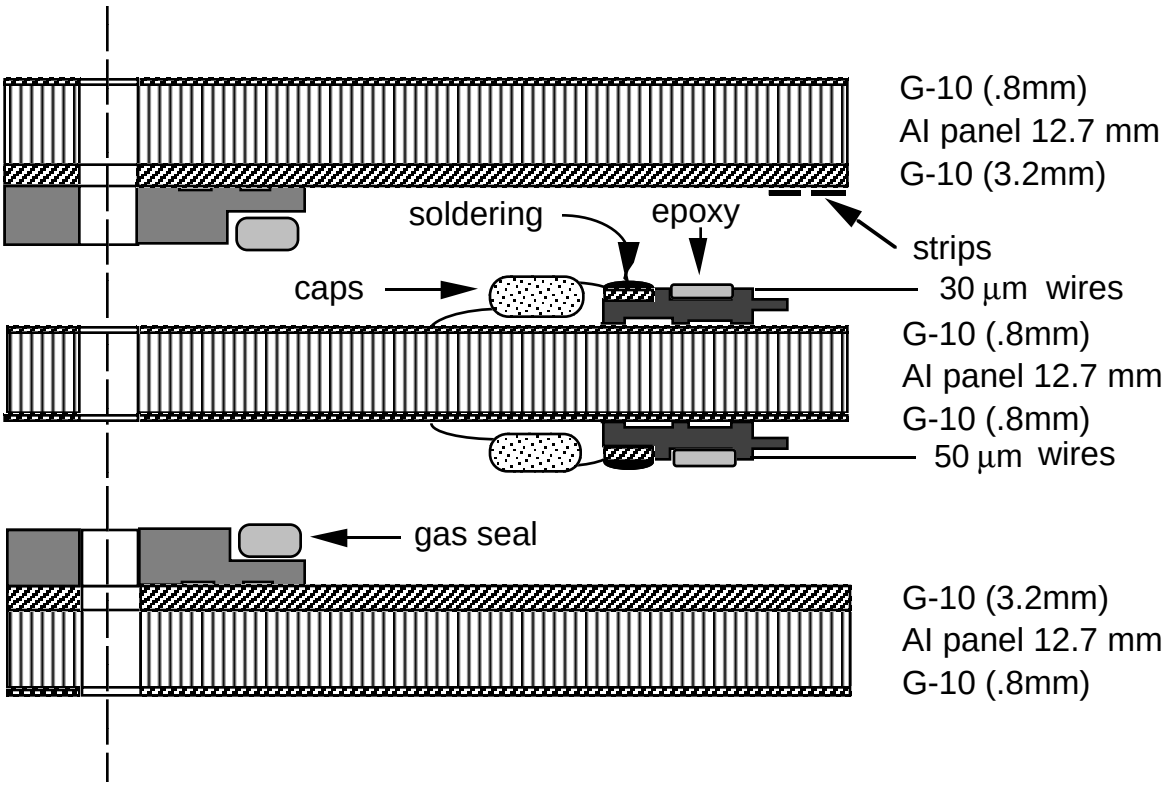

Figure 1: Schematic view of chamber construction.

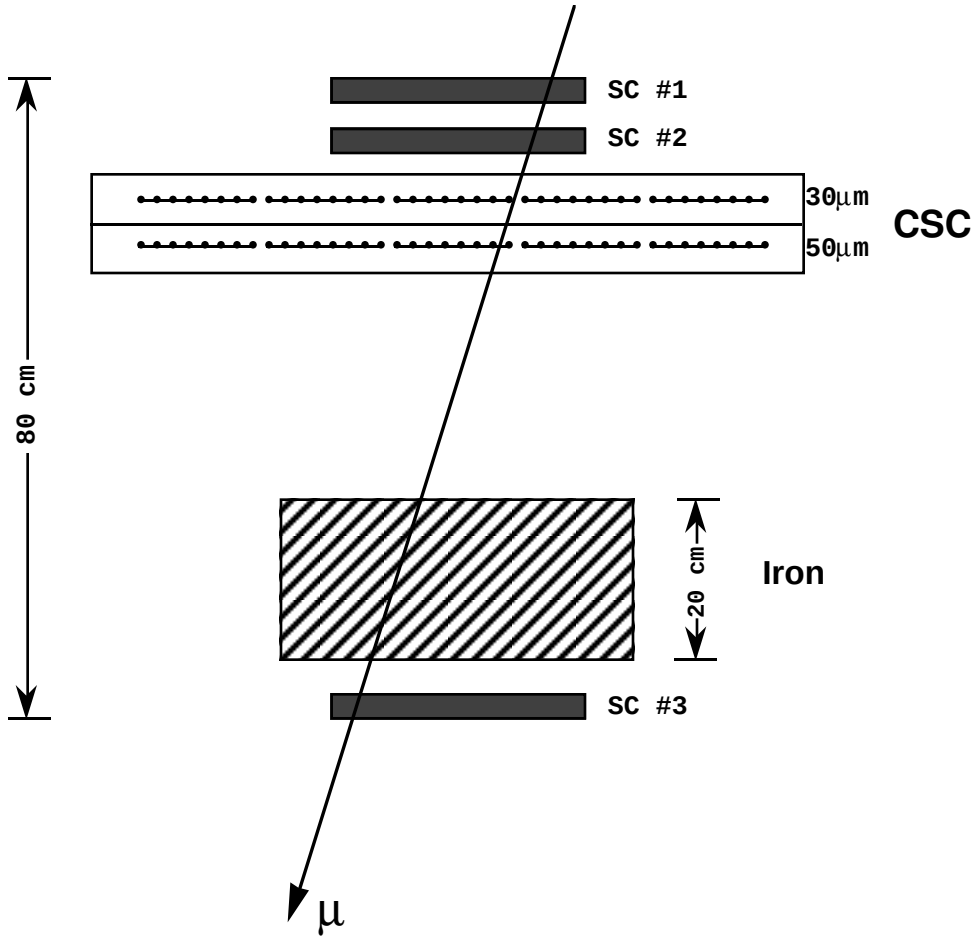

Scintillator Counter Sizes (SC #1-SC#3): *40 cm x 30 cm x 1.5 cm*

Coincidence Count Rate: *0.8 muons/sec*

Figure 2: Schematic view of the experimental set-up.

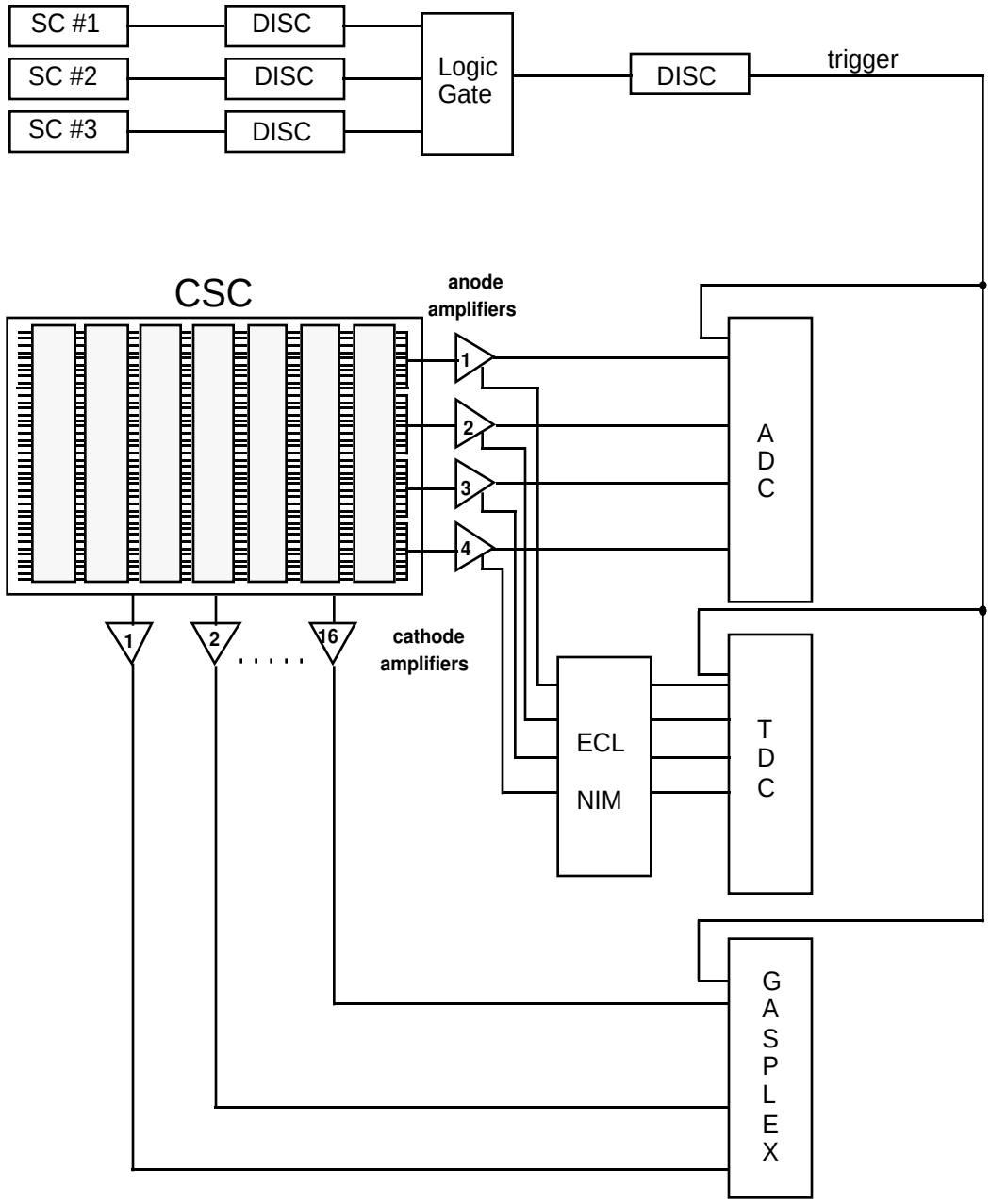

Figure 3: Electronic read-out scheme.

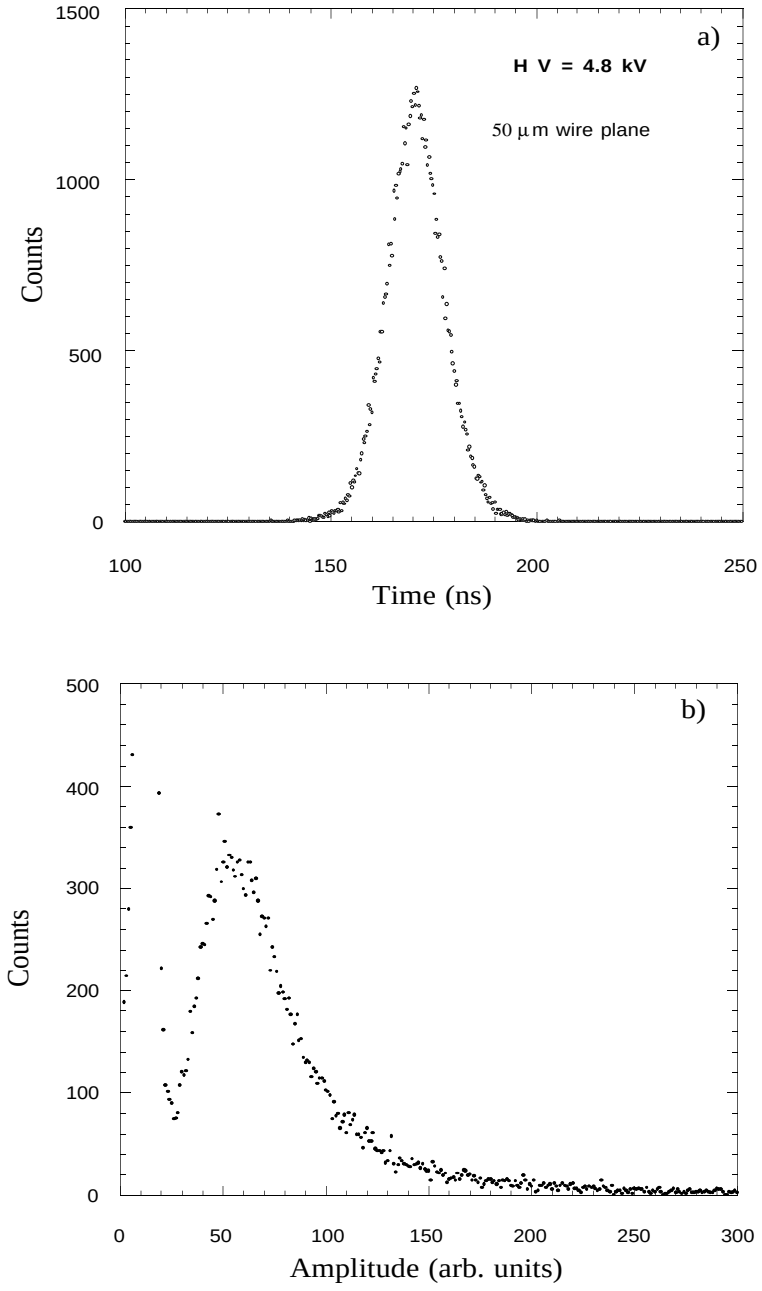

Figure 4: Typical time (a) and amplitude (b) spectrums of the anode signals from cosmic rays.

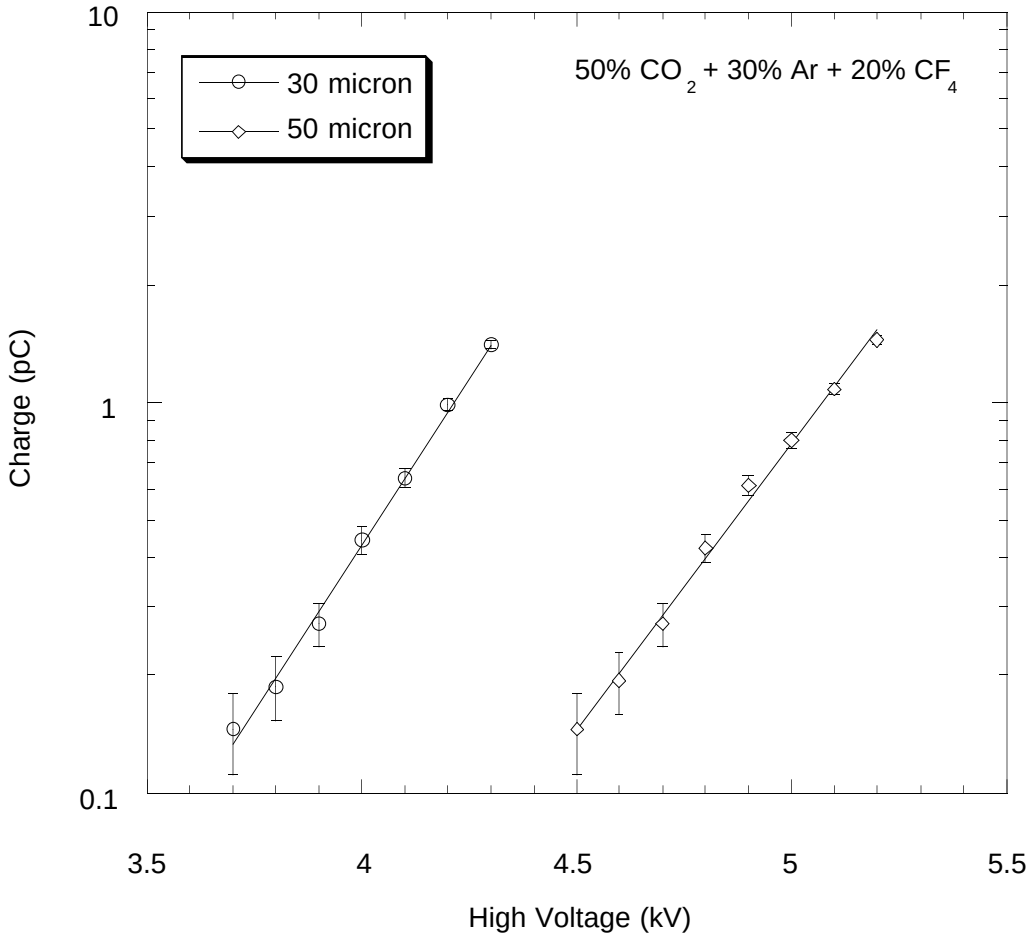

Figure 5: Gas gain in the CSCs.

a)

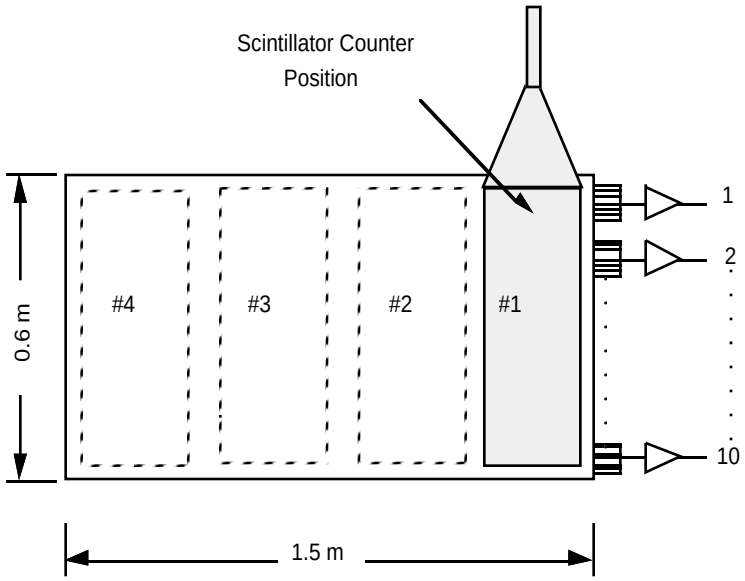

b)

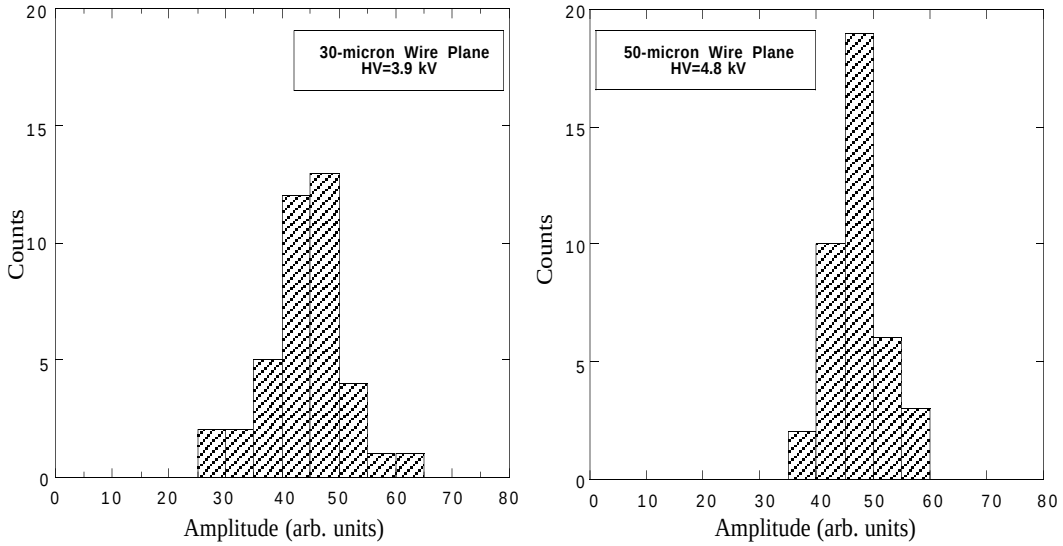

Figure 6: Gas gain uniformity in the CSCs:
a) experimental set-up
b) peak position distributions for different chamber segments of 5 cm x 30 cm.

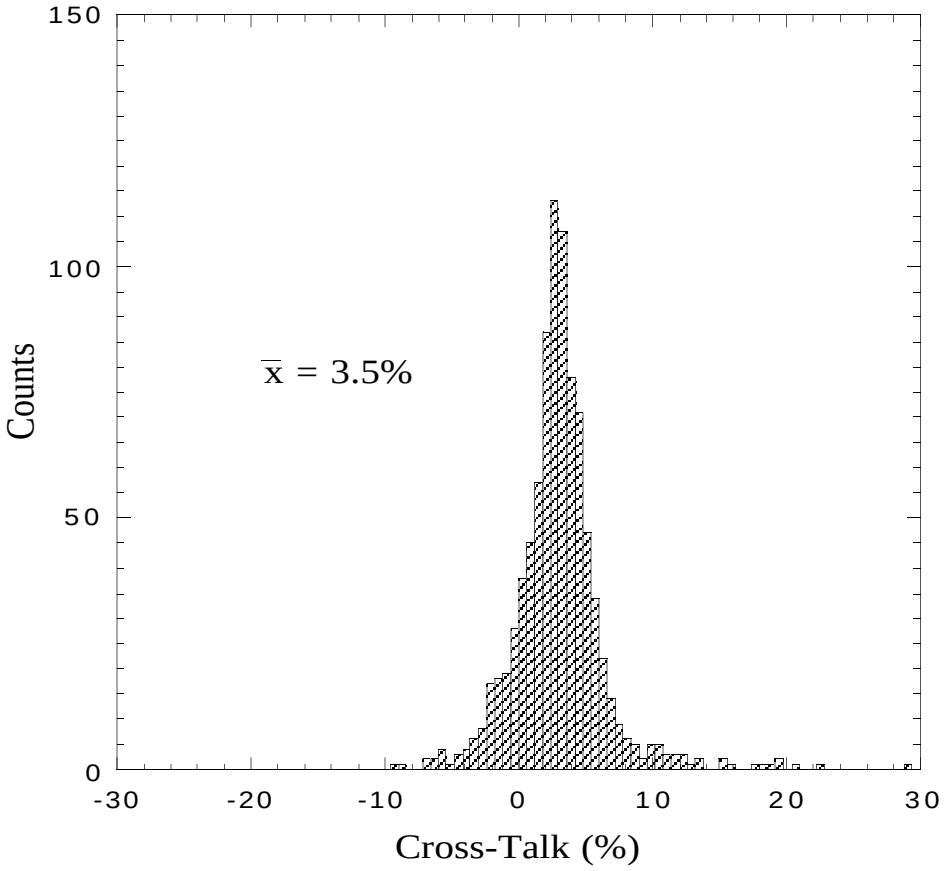

Figure 7: Anode signals cross-talk in the CSC.

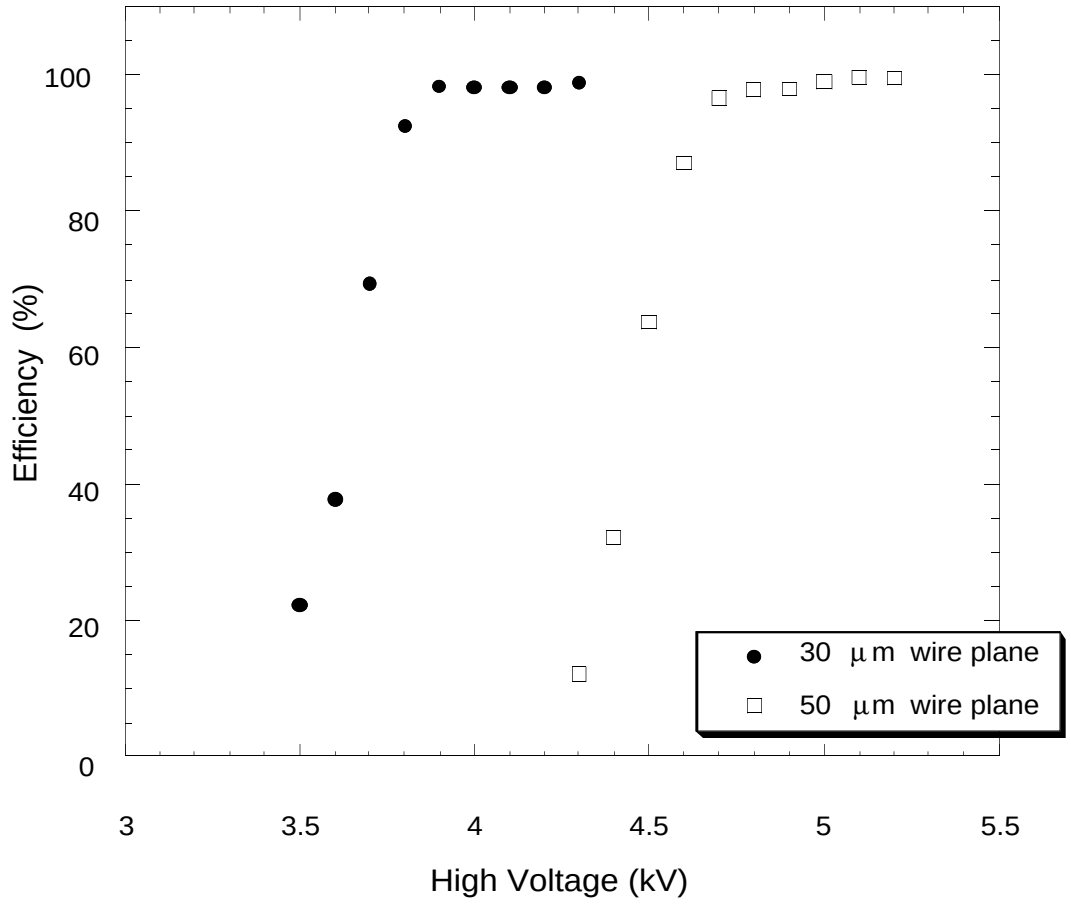

Figure 8: Efficiency of the CSCs.

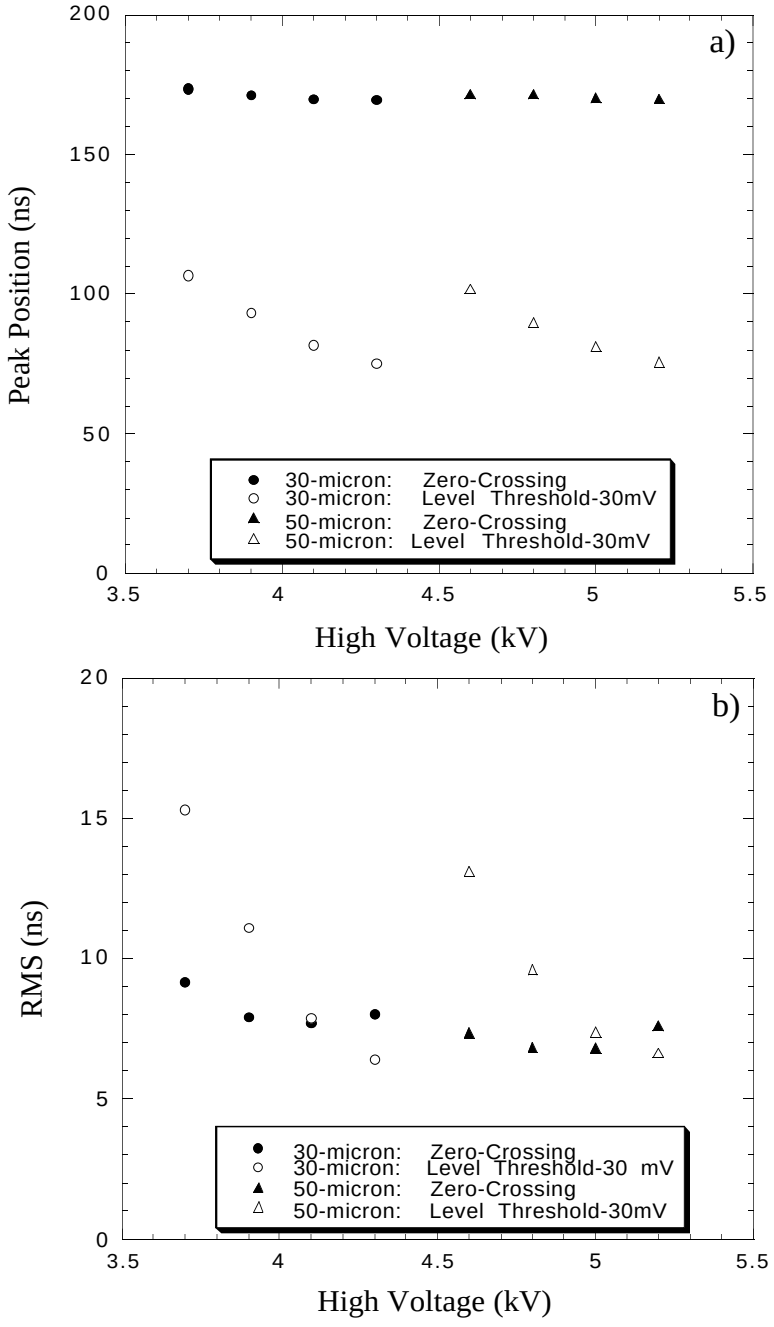

Figure 9: Time characteristics of the CSCs for both discriminator types:
a) peak position
b) time resolution.

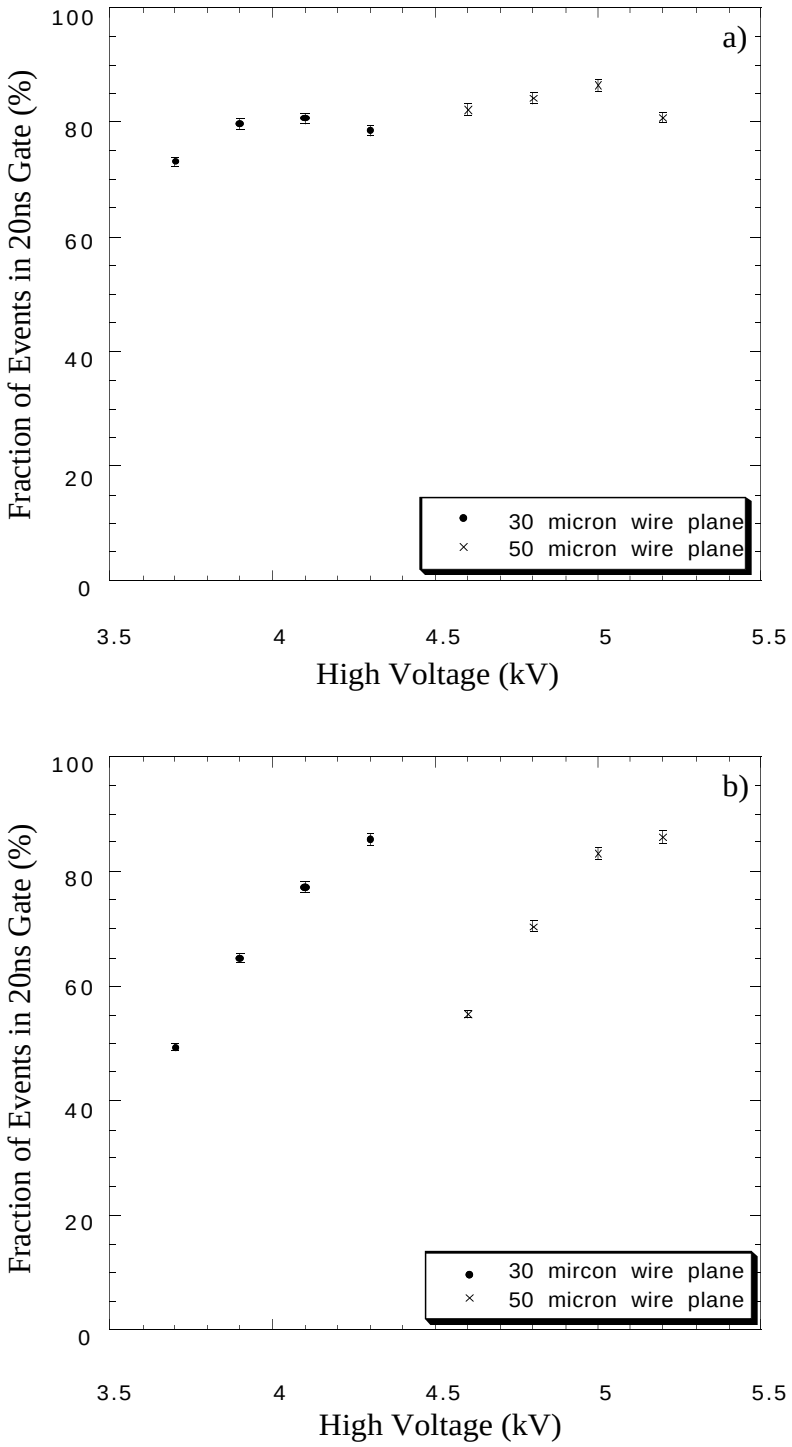

Figure 10: Efficiency for one CSC plane in 20nsec time gate:
a) zero-crossing discriminator
b) leading-edge discriminator.

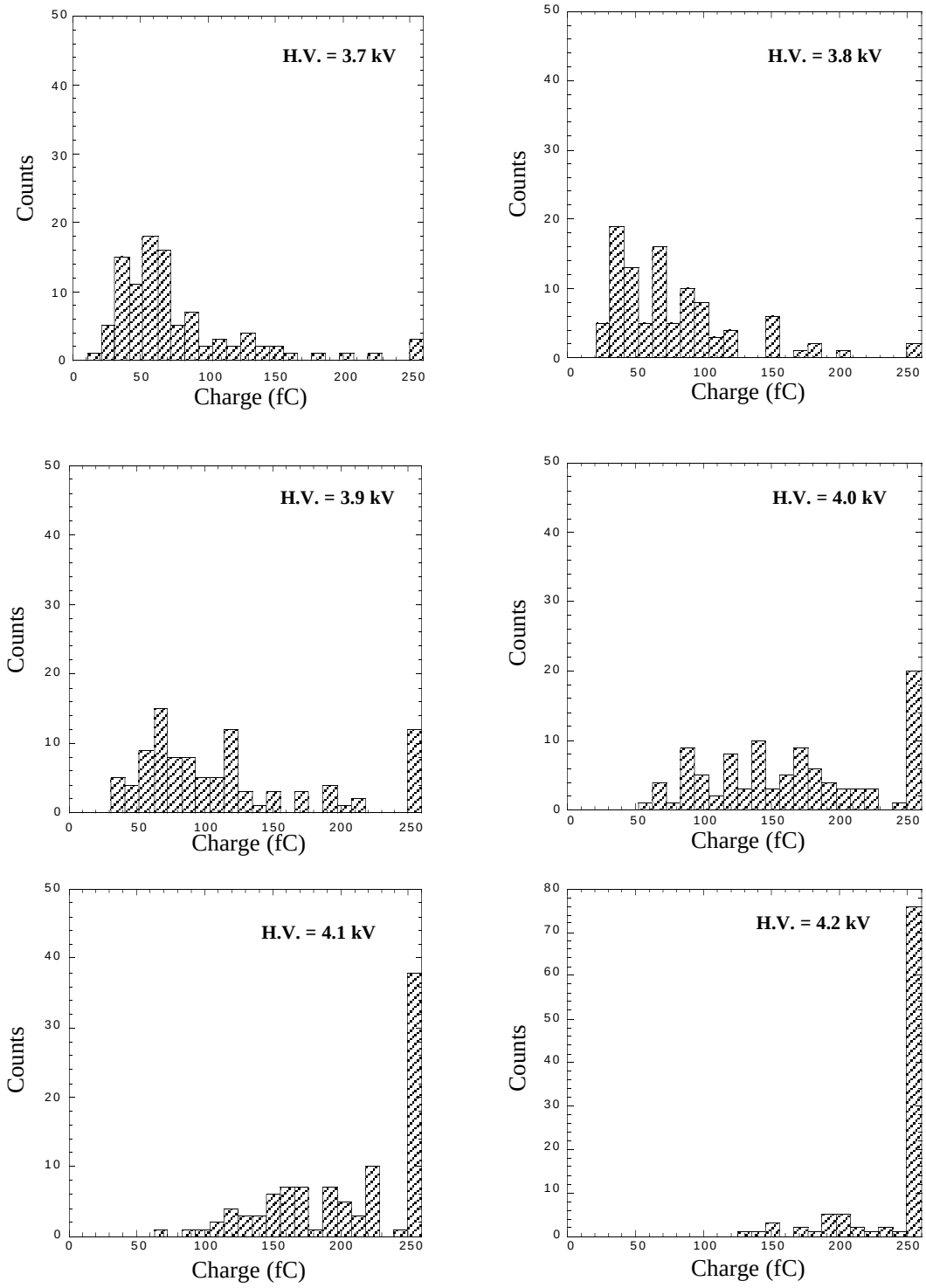

Figure 11: Distribution of the maximum charge from the cathode strips.

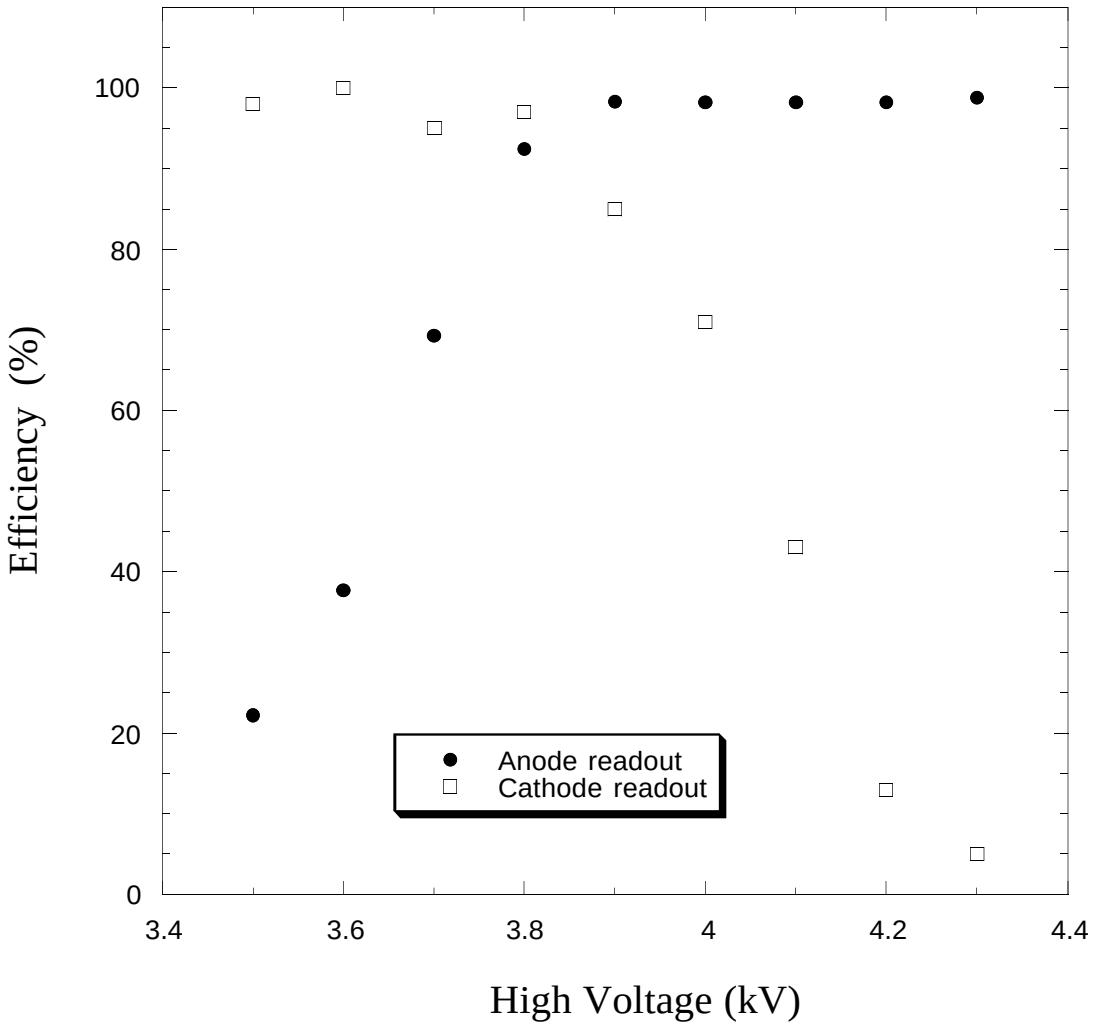

Figure 12: Efficiency of anode and cathode electronics for 30 μm wire plane.